

Subwavelength light localization based on optical nonlinearity and light polarization

Pavel N. Melentiev,¹ Anton E. Afanasiev,¹ Artur A. Kuzin,² Andrey S. Baturin,² and Victor I. Balykin^{1,*}

¹Institute for Spectroscopy Russian Academy of Sciences, Phizicheskaya str. 5, Moscow, Troitsk 142190, Russia

²Moscow Institute of Physics and Technology, Institutskiy per. 9, Dolgoprudny, Moscow Region 141700, Russia

*Corresponding author: balykin@isan.troitsk.ru

Received April 9, 2013; revised May 24, 2013; accepted May 28, 2013;

posted May 31, 2013 (Doc. ID 188536); published June 25, 2013

We propose and experimentally realize subwavelength light localization based on the optical nonlinearity of a single nonlinear element in nanoplasmonics—a split hole resonator (SHR). The SHR is composed of two basic elements of nanoplasmonics, a nanohole, and a nanorod. A peak field intensity occurs at the single spot of the SHR nanostructure. We demonstrate the use of the SHR as a highly efficient nonlinear optical element for (i) the construction of a polarization-ultrasensitive nanoelement and, as a practical application, (ii) the building up of an all-optical display. © 2013 Optical Society of America

OCIS codes: (310.6628) Subwavelength structures, nanostructures; (050.1220) Apertures; (190.2620) Harmonic generation and mixing.

<http://dx.doi.org/10.1364/OL.38.002274>

Focusing a light beam into a subwavelength spot is possible by using different approaches: (1) by an approach based on superoscillation phenomena [1], (2) by using a negative-index metamaterial lens [2], (3) by adiabatic transformation of a plasmonic field [3], (4) by coherent control of ultrafast pulses [4], (5) by using nanoantenna arrays [5], and also (6) by illumination of a plasmonic metamaterial by a plane wave with tailored phase [6].

Here we experimentally demonstrate a different approach to subwavelength light localization. Our approach is based on the strong optical nonlinearity of a particular metal nanostructure, which we call a split hole resonator (SHR) [7], and the polarization of the excitation radiation.

The SHR is composed of a nanorod and a nanohole that are formed in a metal nanofilm [Fig. 1(a)]. The wavelength (1.5 μm) of the incident radiation corresponds to the plasmon resonance of this SHR nanostructure. The calculated spatial distributions of the electric field amplitude [insets in Fig. 1(d)] show specific features of the SHR nanostructure. It can be seen that the SHR forms a true monopole antenna with the field localization near the nanorod tip and that it has advantages compared to monopole nanoantennas of other types [7]. The calculation also shows that the maximal field strength in the SHR is an order of magnitude higher than the field magnitude for the nanorod alone [7].

The peak field in the SHR is much stronger than the peak fields of the nanorod and the nanohole, since the field in the SHR is enhanced by two mechanisms: the surface plasmon resonance excitation and the lightning-rod effect. As has been shown [7], the SHR is also a highly efficient nonlinear optical element.

An SHR can be also considered a nanolocalized radiation source. From this viewpoint, the SHR has a number of merits in comparison with other nanostructures. First, there is no accompanying background of the excitation radiation (which is very high with nanoparticles). Second, the transmission of the radiation through the SHR is significantly higher than through a nanohole of the same size. Third, since the SHR is created in a metal film, it is capable of withstanding a higher intensity of

radiation incident on it than are isolated nanoparticles [8], and, correspondingly, as a nonlinear element, it can be more efficient.

The construction of the SHR nanoelement was performed in aluminum film. The aluminum film was deposited on the surface of ultrathin (40 nm thick) SiO_2 membranes with a low roughness ($< 1.5 \text{ \AA}$) [9], which, in turn, led to a low roughness of metal films adjacent to the membrane. The high quality of the metal surface greatly reduced the parasitic photoluminescence from roughness of the metal surface [10]. For this reason, in all measurements, the smooth side of the films was exposed to the radiation. The SHRs were formed by using a focused ion beam in an aluminum film 100 nm thick. The nanohole diameter is 380 nm [Fig. 1(a)].

Investigations of SHRs were performed using radiation at a wavelength of 1560 nm, since at this wavelength aluminum is characterized by strong optical nonlinear properties; thus the optical nonlinearity coefficient $\chi^{(3)}$ of aluminum is approximately 1000 times higher than that of gold [8]. In addition, the radiation at 1560 nm is widely

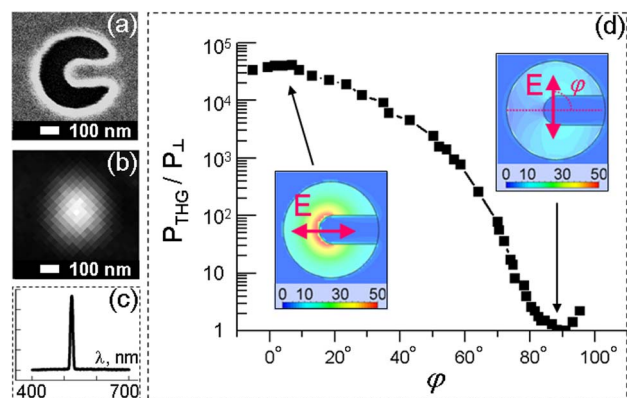


Fig. 1. SHR: (a) electron microscope image of the SHR, (b) optical image of the SHR and detection at the THG wavelength, (c) spectrum of light generated by SHR, and (d) dependence of the THG on the polarization of the excitation radiation. Insets: calculated electric field inside the SHR.

used in telecommunication systems. SHR nanostructures were irradiated by a femtosecond laser (120 fs, repetition rate 70 MHz, power 15 mW). The optical and spectral properties of the SHR were measured by using an inverted microscope (Nikon Eclipse Ti). The laser radiation was focused by an objective (10 \times , NA = 0.25) into a spot with diameter 4.3 μm . The peak radiation intensity on the sample was of the order of 1.1×10^{10} W/cm². The radiation from the SHR was collected with objectives 40 \times , NA = 0.65, or 100 \times , NA = 1.49. A set of interference and color filters was used to suppress the excitation radiation. Finally, the radiation at the fundamental frequency was suppressed by more than 13 orders of magnitude.

First we studied nonlinear optical processes in SHR, such as the third-harmonic generation (THG). We have calculated the spatial distribution of the electric field in the SHR, [Fig. 1(d)]. It can be seen that the spatial distribution of the electric field amplitude at the fundamental frequency has a clearly pronounced single maximum and is localized inside the SHR near the tip of its nanorod. This field acts as a source of a third-order polarization, which results in the THG. Figures 1(b) and 1(c) also present the experimental results for the THG from a single SHR. Details of the measurement of the THG signal from a single SHR can be found in [7]. It can be seen from the figure that the spatial localization of the THG radiation spot is determined by the size of the nanorod tip, which is about 100 nm. In the optical image of the nanostructure obtained at the wavelength of the third harmonic, a diffraction-limited spot is seen, the width at half-height of which is about 230 nm [Fig. 1(b)]. Measurements of the emission spectrum of the SHR nanostructure [Fig. 1(c)] show that it consists of a narrow line located at the frequency of the THG.

Our measurements and calculations showed that the THG efficiency of the SHR nanostructure strongly depends on (1) its geometry, (2) the material of the film, (3) the refractive index of the medium surrounding the SHR, and (4) the laser polarization. This behavior is explained by the well-known strong dependence of the excitation efficiency of localized plasmon oscillations on the geometry of the nanostructure and its local environment, which determines the distribution and amplitude of the electromagnetic field near the nanostructure.

The geometry of the SHR has a clearly pronounced anisotropy, which is determined by the direction of its nanorod. In turn, the presence of anisotropy suggests dependence of the optical response of SHR on the polarization of the incident radiation. We investigated SHR response to the polarization. First, the distributions of the near field were calculated for the polarization directed orthogonally to the nanorod and along it. A change in the near field at the fundamental frequency due to a change in the polarization does not exceed 40 [insets in Fig. 1(d)]. Then the polarization dependence of the SHR nonlinear response was measured [Fig. 1(d)]. It can be seen from this figure that, for the polarization orthogonally to the nanorod, the THG signal is minimal. On rotation of the polarization vector by 90 $^\circ$, the signal at the frequency of the THG increases 40,000 times! This extremely high sensitivity to the polarization is a consequence of the

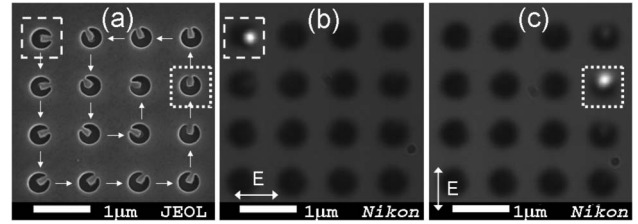


Fig. 2. All-optical display: (a) electron microscope image of the display, (b) and (c) optical images of the display illuminated by radiation polarized in the direction of the nanorods.

third-order dependence of the THG efficiency on the incident radiation intensity.

A strong polarization dependence of the THG of the SHR nanostructure shows that SHRs can be used for important applications in optical sensing and ultrafast optical switching [11,12]. As an example of such an application, we demonstrate the use of SHRs for the creation of the prototype of an all-optical display in which SHRs play the role of pixels. An optical display that we realized is an array of 4×4 identical SHRs with spacing between nearest neighbors of 1 μm (Fig. 2). The nanostructures were prepared in an aluminum film 100 nm thick. The nanorod of each SHR is turned by an angle of 11.5 $^\circ$ with respect to the adjacent one [Fig. 3(a)]. This optical display operates as follows. All the SHRs are illuminated by a femtosecond radiation field at a wavelength of 1560 nm. For the polarization vector directed along the nanorod of one of the SHRs, only this nanostructure of the display proves to be tuned to exact resonance with the field, and precisely this nanostructure becomes an efficient radiation source of THG. Therefore, by choosing a certain direction of the polarization vector of the incident radiation, one can switch on a certain pixel of the display.

Figures 2(b) and 2(c) show the results of the proof-of-principle experiment with the all-optical display. On rotation of the polarization vector of the radiation, it is tuned to resonance with one of the SHR structures of the display, and this SHR becomes a light source at the frequency of the THG. For example, to address the first pixel of the display [in Fig. 2(a)] (this SHR is marked with the dashed square), the polarization vector is directed along the nanorod of this SHR. In this case,

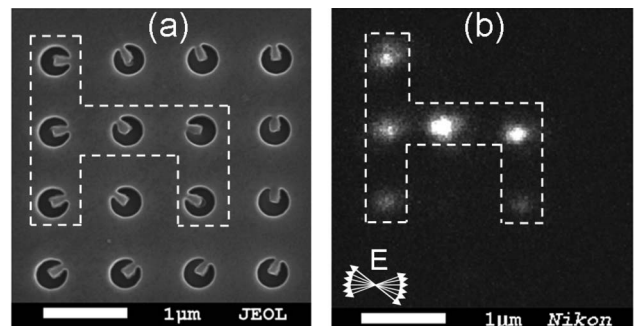


Fig. 3. Image of the letter “h” obtained with an all-optical display: (a) electron microscope image, (b) optical image. The SHRs that are resonant to the excitation radiation are marked by the dashed line. White arrows indicate the polarization of the excitation radiation.

the illumination of the display gives rise to the light emission only from this pixel, as is seen in Fig. 2(b). On rotation of the polarization vector by 90°, the direction of the polarization vector will coincide with the direction of the nanorod of another SHR [in Fig. 2(a), this nanostructure is marked with the dotted square]. In this case, only this pixel is tuned to resonance with the incident radiation, and only it emits light, as is seen in Fig. 2(c).

To observe the functioning of the display (Fig. 2), we used an additional light source (a halogen lamp) to illuminate the display. This illumination allowed us to observe all the SHR nanostructures of the display as dark spots against the background of the signal of scattering from the aluminum film [Figs. 2(b) and 2(c)].

Figure 3(b) presents the simplest image, in the shape of the letter “h,” that was obtained with our optical display. In this demonstration, the polarization was rotated by certain angles to ensure conditions of resonance between the radiation and the required SHR nanostructures of the display. The arrangement of these nanostructures is shown in Fig. 3(a) by the dashed line. As can be seen from Fig. 3(b), the diffraction-limited spots of the radiation at the frequency of the THG form an image of the letter “h.”

We also examined the spatial resolution of the display. It is well known that resonance plasmons of nanostructures are sensitive to their environment and the spacing between them [13]. Our measurements showed that it is possible to independently control the THG on the display with a 500 nm spacing between the SHRs, which is about 1/3 of the wavelength. The measured contrast was about 5 (the light intensity of the excited SHRs divided by that of the unexcited ones).

We would also like to note the possibility of ultrafast control of the pixels of the optical display: relaxation times of plasmon oscillations in aluminum can be as short as about 100 as [14].

In conclusion, we have showed that a SHR nanoplasmonics element allows record efficiency of the THG radiation and that it possesses subwavelength light localization. It makes it possible to realize a nanolocalized radiation source with a spatial localization of about $\lambda/15$. Such a subwavelength light localized source possesses strongly pronounced polarization characteristics. A possible practical application of the SHR is all-optical displays and all-optical chips. Further improvement of the operation efficiency of SHR nanostructures may be

possible by using microcavities based on photonic crystals [10,15,16] or active hyperbolic metamaterials [17].

This work was partially supported by the Russian Foundation for Basic Research, by the Programs of the Presidium of the Russian Academy of Sciences, and by the Ministry of Education and Science of the Russian Federation. The equipment of the CCU ISAN, CCU MIPT was used in this work.

References

1. N. I. Zheludev, *Nat. Mater.* **7**, 420 (2008).
2. J. Valentine, S. Zhang, T. Zentgraf, E. Ulin-Avila, D. A. Genov, G. Bartal, and X. Zhang, *Nature* **455**, 376 (2008).
3. M. I. Stockman, *Phys. Rev. Lett.* **93**, 137404 (2004).
4. M. Aeschlimann, M. Bauer, D. Bayer, T. Brixner, F. J. Garcia de Abajo, W. Pfeiffer, M. Rohmer, C. Spindler, and F. Steeb, *Nature* **446**, 301 (2007).
5. B. Gjonaj, J. Aulbach, P. M. Johnson, A. P. Mosk, L. Kuipers, and A. Lagendijk, *Nat. Photonics* **5**, 360 (2011).
6. T. S. Kao, E. T. F. Rogers, J. Y. Ou, and N. I. Zheludev, *Nano Lett.* **12**, 2728 (2012).
7. P. N. Melentiev, A. E. Afanasiev, A. A. Kuzin, A. S. Baturin, and V. I. Balykin, *Opt. Express* **21**, 13896 (2013).
8. P. N. Melentiev, T. V. Konstantinova, A. E. Afanasiev, A. A. Kuzin, A. S. Baturin, A. V. Tausenev, A. V. Konyaschenko, and V. I. Balykin, *Laser Phys. Lett.* **10**, 075901 (2013).
9. P. N. Melentiev, A. V. Zablotskiy, D. A. Lapshin, E. P. Sheshin, A. S. Baturin, and V. I. Balykin, *Nanotechnology* **20**, 235301 (2009).
10. P. N. Melentiev, A. E. Afanasiev, A. A. Kuzin, A. V. Zablotskiy, A. S. Baturin, and V. I. Balykin, *Opt. Express* **19**, 22743 (2011).
11. J. Elliott, I. I. Smolyaninov, N. I. Zheludev, and A. V. Zayats, *Opt. Lett.* **29**, 1414 (2004).
12. R. Gordon, A. G. Brolo, A. McKinnon, A. Rajora, B. Leathem, and K. L. Kavanagh, *Phys. Rev. Lett.* **92**, 037401 (2004).
13. N. Feth, M. König, M. Husnik, K. Stannigel, J. Niegemann, K. Busch, M. Wegener, and S. Linden, *Opt. Express* **18**, 6545 (2010).
14. M. I. Stockman, M. F. Kling, U. Kleineberg, and F. Krausz, *Nat. Photonics* **1**, 539 (2007).
15. P. N. Melentiev, T. V. Konstantinova, A. E. Afanasiev, A. A. Kuzin, A. S. Baturin, and V. I. Balykin, *Opt. Express* **20**, 19474 (2012).
16. P. N. Melentiev, A. E. Afanasiev, A. A. Kuzin, A. V. Zablotskiy, A. S. Baturin, and V. I. Balykin, *J. Exp. Theor. Phys.* **115**, 185 (2012).
17. X. Ni, S. Ishii, M. D. Thoreson, V. M. Shalaev, S. Han, S. Lee, and A. V. Kildishev, *Opt. Express* **19**, 25242 (2011).